Conductive and Highly Catalytic Nanocage for Assembly and Improving Function of Enzyme

Shuo Wu, Jie Wu, Yiying Liu, and Huangxian Ju*

Key Laboratory of Analytical Chemistry for Life Science (Ministry of Education of China), School of Chemistry and Chemical Engineering, Nanjing University, Nanjing 210093, P. R. China

Received August 8, 2007. Revised Manuscript Received November 15, 2007

A conductive nanocage composed of PdNPs-doped (PdNPs = palladium nanoparticles) mesocellular carbon−silica foam was prepared using a designed wet chemical process followed by electrochemical reduction. This nanocage possessed a 3-D interconnected bottleneck mesostructure with large surface area, narrow and controllable pore-size distribution, good biocompatibility, and favorable conductivity and hydrophilicity. The produced PdNPs dispersed homogeneously on the mesowalls and provided the nanocage with a high degree of catalytic ability for the electrooxidation of hydrogen peroxide at an extremely low overpotential, and they offer the possibility to selectively detect oxidase substrates. The nanocage was size-controllable and could be used for volume-selective entrapment of enzymes without aggregation and a change of structure, which preserved good bioactivity of the entrapped enzyme and produced a highly sensitive biosensor with excellent operational and storage stability. Using glucose oxidase as a model, the as-prepared biosensor showed an increase of 130 times in amperometric response due to the presence of PdNPs. The use of the nanocage for enzyme immobilization with excellent catalytic activity of PdNPs will open new horizons for biosensing and biomicroreactor fabrication.

Introduction

The design of highly effective biocatalysts has long attracted considerable interest for bioengineering, biosensor and bioreactor design, and chemical synthesis.[1] One approach extensively used to prepare the biocatalysts is to immobilize natural enzymes on supports. However, the denaturation, aggregation, or limited stability of the immobilized enzymes impairs their performance and makes them rarely adequate for commercially viable processes.[2] Thus, the design of suitable support matrices and a credible immobilization method is a crucial topic.[3,4]

Although silica sol–gels have been used to encapsulate a wide variety of biomolecules, the enzyme loading in conventional sol–gel protocols is usually limited to 0.1–5% (w/w) as the result of protein aggregation at elevated concentrations.[5] Covalent capture can avoid the aggregation; however, this can cause active sites to become unavailable or even prompt denaturation of the protein.[6] Recently, mesoporous materials with straight channels have been prepared for protein immobilization.[7–12] The large surface areas, high pore volumes, and well-ordered pore size distributions of mesoporous materials can avoid the aggregation of proteins.[7] In the early stages, small global proteins with a diameter less than 5 nm were first entrapped in the mesopores due to the limitation of their small pore sizes.[8] After the mesoporous silica materials with pore sizes larger than 10 nm were prepared,[9–12] some big proteins, such as catalase (10.4 nm), were also entrapped in mesoporous materials.[10,12] These works suggested that the materials with large mesopore sizes can improve the immobilization rate and enhance enzyme loading, and that the pore size has a significant influence on the rate of enzyme immobilization.[12] Besides, protein leakage from the straight channels was also unavoidable. Thus, some effective methods including subsequent coating of nanoscale multilayer shells on the protein-loaded mesoporous silica and cross-linking the enzymes in the mesopores have been proposed to prevent the leakage of protein from the mesopores,[4,11,12] and 3-D interconnected mesocellular foams with a bottleneck mesostructure composed of either carbon[4,13] or silica[14] with global mesocells have also been used as supports for the preparation of

* Corresponding author. Tel.: +86(25) 83593593. Fax: +86(25) 83593593. E-mail: hxju@nju.edu.cn.

(1) Schmid, A.; Dordick, J. S.; Hauer, B.; Kiener, A.; Wubbolts, M.; Witholt, B. *Nature* **2001**, *409*, 258–268.
(2) Fox, R. J.; Davis, S. C.; Mundorff, E. C.; Newman, L. M.; Gavrilovic, V.; Ma, S. K.; Chung, L. M.; Ching, C.; Tam, S.; Muley, S.; Grate, J.; Gruber, J.; Whitman, J. C.; Sheldon, R. A.; Huisman, G. W. *Nat. Biotechnol.* **2007**, *25*, 338–344.
(3) Patel, A.; Li, S. X.; Yuan, J. M.; Wei, Y. *Nano Lett.* **2006**, *6*, 1042–1046.
(4) Lee, J.; Lee, D.; Oh, E.; Kim, J.; Kim, Y. P.; Jin, S.; Kim, H. S.; Hwang, Y.; Kwak, J. H.; Park, J. G.; Shin, C. H.; Kim, J.; Hyeon, T. *Angew. Chem., Int. Ed.* **2005**, *44*, 7427–7432.
(5) Luckarift, H. R.; Spain, J. C.; Naik, R. R.; Stone, M. O. *Nat. Biotechnol.* **2004**, *22*, 211–213.
(6) Doerr, A. *Nat. Methods* **2005**, *2*, 642–643.
(7) Ravindra, R.; Zhao, S.; Gies, H.; Winter, R. *J. Am. Chem. Soc.* **2004**, *126*, 12224–12225.
(8) Hartmann, M. *Chem. Mater.* **2005**, *17*, 4577–4593.
(9) Zhang, H.; Sun, J. M.; Ma, D.; Bao, X. H.; Klein-Hoffmann, A.; Weinberg, G.; Su, D. S.; Schlög, R. *J. Am. Chem. Soc.* **2004**, *126*, 7440–7441.
(10) Wang, Y. J.; Caruso, F. *Chem. Commun.* **2004**, 1528–1529.
(11) Wang, Y. J.; Caruso, F. *Adv. Mater.* **2006**, *18*, 795–800.
(12) Wang, Y. J.; Caruso, F. *Chem. Mater.* **2005**, *17*, 953–961.
(13) Lee, D.; Lee, J.; Kim, J.; Kim, J.; Na, H. B.; Kim, B.; Shin, C. H.; Kwak, J. H.; Hyeon, T.; Kim, H. S. *Adv. Mater.* **2005**, *17*, 2828–2833.
(14) Han, Y.; Lee, S. S.; Ying, J. Y. *Chem. Mater.* **2006**, *18*, 643–649.

10.1021/cm702906c CCC: $40.75
Published on Web 12/28/2007

biocatalysts. However, the silica mesocellular foam suffers from poor conductivity to limit the electron transfer, while the carbon mesocellular foam has the disadvantage of poor hydrophilicity, which makes the approach of the active enzyme sites by substrates in aqueous solution difficult. Our previous work suggested a mesocellular carbon−silica hybrid foam (MSCF) for the immobilization of glucose oxidase (GOD),[15] but the obtained biocatalyst or biosensor suffers from poor sensitivity due to the low catalytic efficiency. This work designs a conductive and highly catalytic nanocage with suitable window size and hydrophilicity to size-selectively entrap enzyme molecules and suggests a novel approach to assembling enzymes in a nanocage, which increases greatly the enzyme accessibility needed for achieving fast response and a high degree of catalytic activity. The palladium nanoparticles (PdNPs) deposited in the nanocage improve the catalytic efficiency of the resulting biocatalyst by decreasing extremely the oxidation overpotential of hydrogen peroxide and also improve the interaction between GOD and the mesowalls through interaction with the nitrogen groups[16] such as amine groups or amide in the amino acid residues of GOD. This work opens new avenues for the immobilization of enzymes, preparation of highly effective biocatalysts, and highly sensitive and selective detection of oxidase substrates.[17]

Experimental Section

Reagents. Furfuryl alcohol was purchased from Fluka (Germany). Poly(ethylene oxide)-block-poly(propylene)-block-poly(ethylene oxide) ($EO_{20}PO_{70}EO_{20}$) was purchased from BASF (Germany). Glucose oxidase (type II-S, 39.8 U/mg), β-D-(+)-glucose, Nafion, horseradish peroxidase, *o*-dianisidine, and 1,3,5-trimethylbenzene were purchased from Sigma-Aldrich, Inc. (U. S. A.). All other reagents were of analytical grade and used without further purification. A 0.2 M phosphate buffer solution (PBS) was prepared by mixing the stock solutions of NaH_2PO_4 and Na_2HPO_4. A 0.05 M NaAc-HCl buffer solution was prepared by dissolving sodium acetate in water and adjusted with 1 M HCl to pH 5.1. Doubly distilled water was used in all experiments.

Synthesis of MSCF and Pd^{2+}-MSCF. MSCF was prepared according to the method reported previously.[15] The pore size dimension was tailored by adjusting the ratio of two templates during the preparation procedure. Pd^{2+}-MSCF was formed using a cationic exchange process, which was performed by dispersing 4.0 mg of MSCF in 2.0 mL of a $PdCl_2$ solution and stirring for 10 h. The terms $_{0.05}Pd^{2+}$-MSCF, $_{0.25}Pd^{2+}$-MSCF, and Pd^{2+}-MSCF refer to the materials exchanged with the initial Pd^{2+} concentrations of 0.05, 0.25, and 5.0 mM, respectively.

Entrapment of GOD in Pd^{2+}-MSCF. For characterization, 5.0 mg of Pd^{2+}-MSCF was added in 2.0 mL of GOD solutions with different concentrations. The resulting mixtures were continuously shaken at room temperature for 24 h to obtain GOD-entrapped Pd^{2+}-MSCF. The amount of entrapped GOD could be measured with UV absorption at 280 nm by subtracting the amount found in the supernatant solution before and after GOD entrapment. The GOD-entrapped Pd^{2+}-MSCF sample for N_2 sorption analysis was prepared by dispersing 0.12 g of the Pd^{2+}-MSCF in 30 mL of a 4.0 mg/mL GOD solution, and the mixture was continuously shaken for 4 h followed by centrifugation to remove the free protein.

Preparation of Pd-MSCF and GOD-Entrapped Pd-MSCF-modified Electrodes. Homemade graphite electrodes (GE; 3.0 mm in diameter) were used for the deposition of PdNPs in MSCF, which were first polished to a mirror finish with 0.3 and 0.05 mm alumina slurries (Beuhler) followed by thorough rinsing with deionized water. After successive sonication in 1:1 nitric acid/acetone and deionized water, the electrodes were rinsed with deionized water and dried at room temperature. A total of 12 mg of MSCF, $_{0.05}Pd^{2+}$-MSCF, $_{0.25}Pd^{2+}$-MSCF, and Pd^{2+}-MSCF was added into 3.0 mL of water and stirred for 2 h to get their suspensions with a concentration of 4.0 mg/mL. A total of 2.5 μL of the suspension and 3.0 μL of 0.5% Nafion was subsequently dropped on the pretreated GE surface and allowed to dry in the air for 2 h after each dropping to get the MSCF-, $_{0.05}Pd^{2+}$-MSCF-, $_{0.25}Pd^{2+}$-MSCF-, and Pd^{2+}-MSCF-modified electrodes.

The MSCF and the Pd^{2+}-MSCF-modified electrodes were first immersed in GOD solution (3.0 mg/mL in a NaAc-HCl buffer solution at pH 5.1) for 140 min at 4 °C for GOD entrapment. The Pd^{2+} adsorbed on the mesowalls of MSCF was reduced at an applied potential of −0.5 V for 300 s in a N_2-saturated 0.1 M KCl solution for the production of PdNP-deposited MSCF. The corresponding electrodes were named $_{0.05}$Pd-MSCF-, $_{0.25}$Pd-MSCF-, Pd-MSCF-, and GOD/Pd-MSCF-modified electrodes. For TEM and EDX characterization, Pd-MSCF was obtained by scratching after the electrochemical reduction was finished.

Activity Assay of GOD. The activity assay of GOD was performed following instructions from Sigma. A total of 2.0 mL of a 5.0 mg/mL GOD PBS solution (pH 7.0) was stored at room temperature. For each detection, 5.0 mL of GOD solution was diluted to 0.8 unit/mL with an acetate buffer at pH 5.1, then its activity was monitored by spectrophotometric measurement.

Results and Discussion

Characterization of the Pd-MSCF and Pd^{2+}-MSCF. The transmission electron micrograph (TEM, Figure 1A) demonstrated the formation of PdNPs (black dots) with sizes of 1–3 nm on the mesowalls. The corresponding energy-dispersive X-ray spectrum (EDXS; Figure 1B) showed the peak of palladium at 2.85 keV, which indicated a palladium content of 6.1%. This value was in good agreement with the result of 6.57% obtained from inductively coupled plasma analysis. The latter was detected in the whole sample range, indicating a homogeneous dispersion of the PdNPs on the mesowalls. The crystalline structure of the deposited PdNPs was characterized by the X-ray diffraction pattern. As shown in Figure 2, three well-resolved peaks centered at 2θ values of 40.16°, 46.76°, and 68.32° were observed on the Pd-MSCF, which were attributed to the 111, 200, and 220 diffractions of the typical face-centered-cubic crystalline structure of palladium.[18]

The surface area and pore volume of as-prepared MSCF were measured to be 242 m^2/g and 1.01 cm^3/g from its nitrogen sorption isotherm (Figure 3A). Upon the exchange process between Pd^{2+} in solution and the protons on mesowalls of MSCF, these parameters decreased to 219 m^2/g and 0.91 cm^3/g, respectively. The shape of the isotherm did

(15) Wu, S.; Ju, H. X.; Liu, Y. *Adv. Funct. Mater.* **2007**, *17*, 585–592.
(16) Drelinkiewicza, A.; Hasikb, M.; Quillardc, S.; Paluszkiewiczb, C. *J. Mol. Struct.* **1999**, *511–512*, 205–215.
(17) You, T.; Niwa, O.; Tomita, M.; Hirono, S. *Anal. Chem.* **2003**, *75*, 2080–2085.
(18) Hana, P.; Wang, X. M.; Qiu, X. P.; Ji, X. L.; Gao, L. X. *J. Mol. Catal. A: Chem.* **2007**, *272*, 136–141.

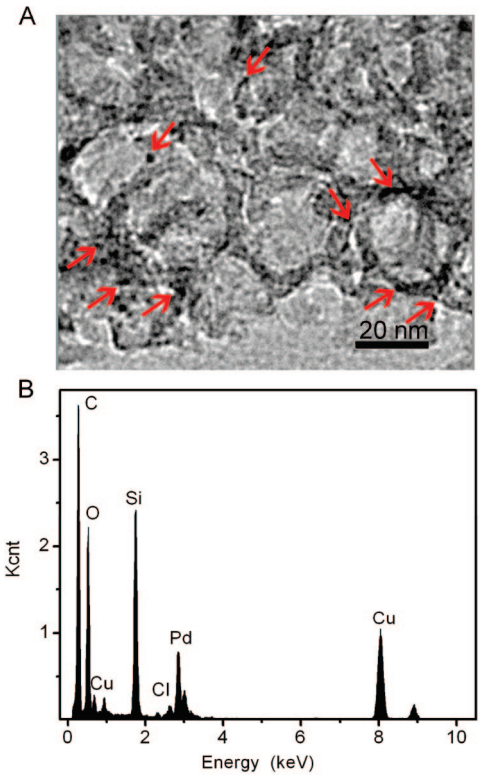

Figure 1. Morphology and composition of Pd-MSCF. (A) TEM of Pd-MSCF. (B) EDXS of Pd-MSCF. The Cu peak resulted from the sample support for TEM measurements.

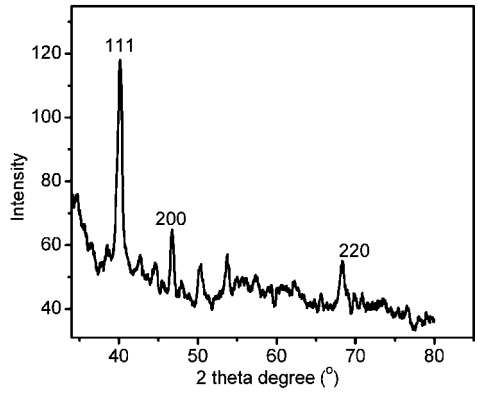

Figure 2. X-ray diffraction pattern of Pd-MSCF.

not change after the exchange of Pd^{2+} cations (Figure 3A), suggesting the good maintenance of the mesostructure and the uniform coverage of Pd^{2+} cations on the mesowalls, which showed little influence on the pore size distribution of the MSCF. The pore size distributions (Figure 3B) were calculated from the adsorption and desorption branches of the isotherms using the Barrett–Joyner–Halenda method. Both MSCF and Pd^{2+}-MSCF displayed two main kinds of mesopores centered at 9 and 20 nm, respectively, indicating an ink-bottle-like porous structure.[14] The window size matched well with the dimensions of GOD (5.2 × 6.0 × 7.7 nm),[19] suggesting that Pd^{2+}-MSCF could be applied as a nanocage for the entrapment of GOD.

(19) Hecht, H. J.; Kalisz, H. M.; Hendle, J.; Schmid, R. D.; Schomburg, D. *J. Mol. Biol.* **1993**, *229*, 153–172.

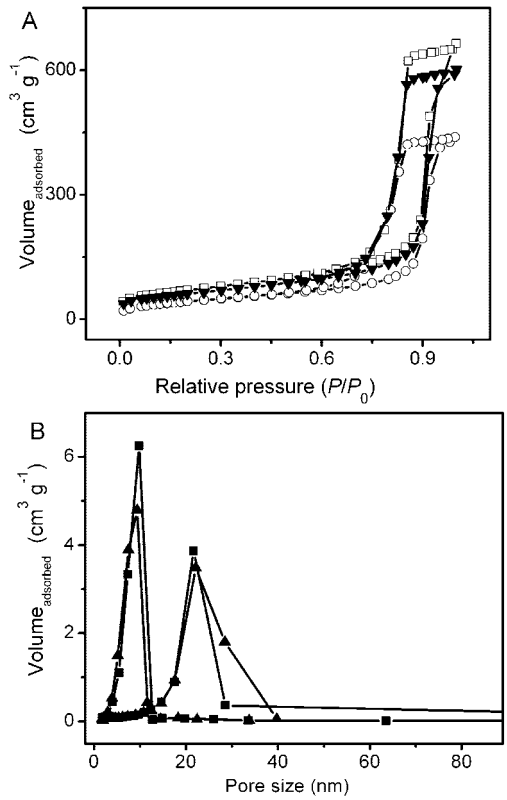

Figure 3. (A) Nitrogen sorption isotherms of MSCF (□), Pd^{2+}-MSCF (▼), and GOD/Pd^{2+}-MSCF (○) and (B) pore size distribution of MSCF (■) and Pd^{2+}-MSCF (▼).

Electrocatalytic Behavior of the Pd-MSCF. After electrochemical reduction, the PdNPs formed on the mesowalls showed high catalytic activity toward H_2O_2 oxidation, as shown in Figure 4A. At the Pd-MSCF-modified electrode, the anodic oxidation of H_2O_2 occurred at +0.25 V, while it occurred at potentials more positive than +0.51 V at the MSCF-modified electrode. Obviously, the presence of PdNPs made the oxidation overpotential decrease to 260 mV. The amperometric response of the Pd-MSCF-modified electrodes to 1.0 mM H_2O_2 in PBS at +0.3 V and pH 7.0 was 24.3 μA, comparing with the value of 0.201 μA obtained at the MSCF-modified electrode; the doping of PdNPs on MSCF improved the amperometric response to H_2O_2 oxidation by more than 120 times (Figure 4B), further proving the high catalytic ability of the PdNPs.

The catalytic ability of PdNPs depended on the amount of palladium doped on the mesowalls. With the increasing initial concentration of Pd^{2+} for the exchange process, which meant the increasing amount of PdNPs doped on the mesowalls of MSCF, the amperometric response to H_2O_2 oxidation at +0.3 V increased and reached a maximum response at the initial Pd^{2+} concentration of 5.0 mM (Figure 5A). The maximum response did not change when more palladium was deposited at the Pd-MSCF-modified electrode by electrochemical reduction of Pd^{2+} in a N_2-saturated 0.25 mM $PdCl_2$ + 0.1 M KCl solution at a reduction current of 50 μA for different periods (Figure 5B), suggesting the saturated exchange between Pd^{2+} and the proton and the maximum deposition.

Entrapment of GOD into Pd^{2+}-MSCF. The highly sensitive response to H_2O_2 showed the potential application

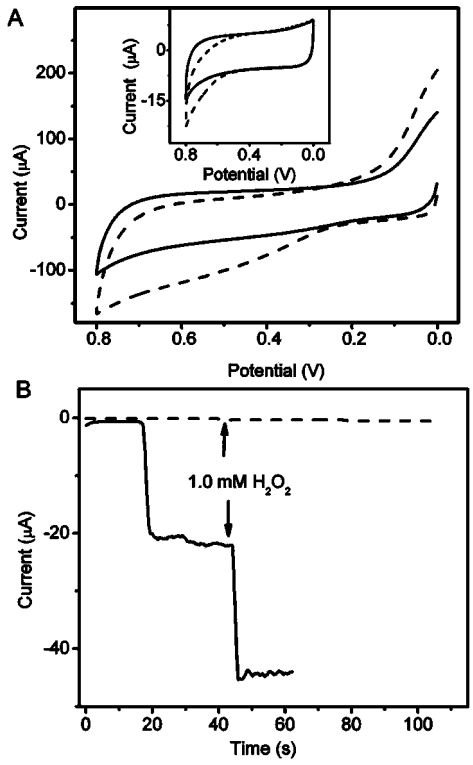

Figure 4. (A) Cyclic voltammograms of Pd-MSCF- and MSCF- (inset) modified electrodes in 0.2 M PBS (pH 7.0) in the absence (solid) and presence (dash) of 3.0 mM H_2O_2. (B) Amperometric responses of the MSCF- (dash) and Pd-MSCF- (solid) modified electrodes to 1.0 mM H_2O_2 in 0.2 M PBS at +0.3 V.

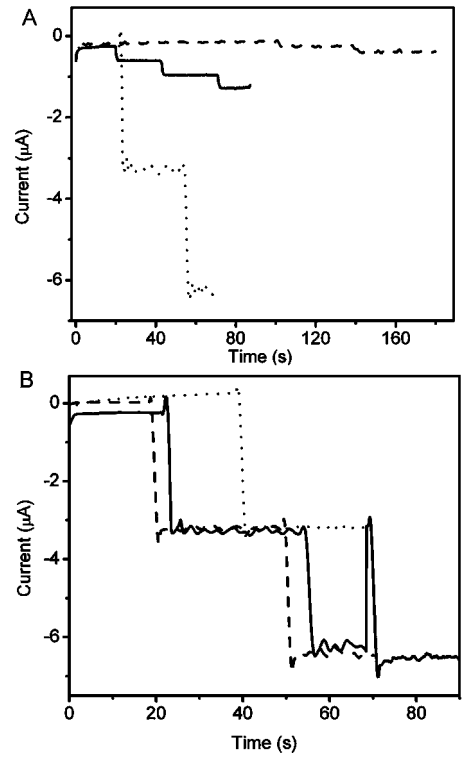

Figure 5. Amperometric responses of $_{0.05}$Pd-MSCF- (dash), $_{0.25}$Pd-MSCF- (solid), and Pd-MSCF- (dot) modified electrodes (A) and a Pd-MSCF-modified electrode with further electrodeposition of palladium in a N_2-saturated 0.25 mM $PdCl_2$ + 0.1 M KCl solution at a reduction current of 50 μA for 0 (solid), 100 (dash), and 200 (dot) seconds (B) to 0.10 mM H_2O_2 in 0.2 M PBS at +0.3 V.

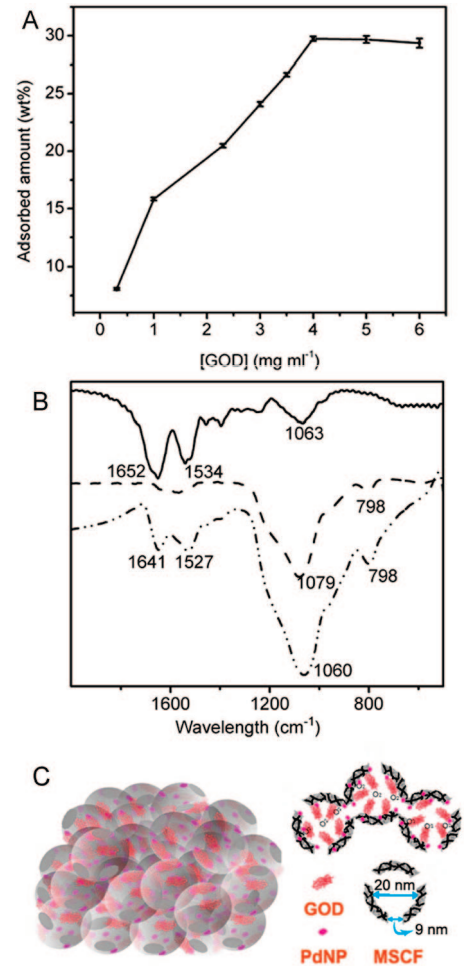

Figure 6. (A) Isotherm of GOD entrapment into Pd^{2+}-MSCF in a NaAC-HAC buffer solution at pH 5.1. (B) IR spectra of pure GOD (solid), Pd^{2+}-MSCF (dash), and GOD-loaded Pd^{2+}-MSCF (dash dot dot). (C) Scheme of GOD assembled in a nanocage.

of the conductive and highly catalytic nanocage in the preparation of biocatalysts for the detection of oxidase substrates. Considering the good match of its window size with the dimension of GOD, it was applied for the selective entrapment of GOD. Figure 6A shows the entrapment capacity of GOD into the nanocage. The loading amount of GOD increased with the increasing GOD concentration until a maximum loading amount of 0.297 ± 0.002 g per gram of Pd^{2+}-MSCF ($n = 3$) was reached, which occurred at a GOD concentration of 4.0 mg/mL. The maximum loading value meant that the number of molecules of GOD entrapped in the mesopores was 1.12×10^{18}/g. From the pore volume of 0.91 cm^3/g and the pore diameter of 20 nm, the pore number could be approximately calculated to be 2.2×10^{17}/g assuming the volume of the bottleneck was neglected. Thus, the maximum number of GOD molecules entrapped in each mesopore of MSCF was about five. After the entrapment of GOD in the nanocage, the nitrogen sorption isotherm decreased significantly (Figure 3A), and the mesopore volume decreased from 0.91 to 0.66 cm^3/g, further proving the entrapment of GOD into the nanocage. In addition, the inner surface area of one nanocage was calculated approximatively from the nitrogen sorption surface area and pore volume to be 1256 nm^2. Although the exact surface area of

the entire nanocage for protein loading was not available, such an inner surface was large enough for a separate array of five GOD molecules, which needed a total surface area of less than 231 nm^2.

Although the entrapment capacity of 29.7% (w/w, GOD/Pd^{2+}-MSCF) for GOD in the nanocage was smaller than 53% (w/w, carbon) for GOD-immobilized magnetic mesocellular carbon foam with a cross-linking process,[4] it was much larger than those obtained at biosilica nanospheres (20%)[5] and other mesoporous materials with small mesopores, such as CMK-3 (0.7%) and active carbon (8.2%),[13] indicating that Pd^{2+}-MSCF was effective for GOD immobilization. In addition, the nanocage could well maintain the structure of the entrapped GOD. Figure 6B shows the IR spectra of different materials. The exchange between Pd^{2+} and protons of surface silanol groups led to a blue shift of the silanol adsorption peak from 1070[15] to 1079 cm^{-1}. After GOD molecules were entrapped in the nanocage, the adsorption peak shifted from 1079 to 1060 cm^{-1}, indicating the interaction between the negatively charged groups of GOD and the Pd^{2+}-modified mesowalls. The absorption peaks centered at 1641 and 1527 cm^{-1} for the GOD-loaded nanocage were attributed to the typical absorptions of amide I and amide II in the protein molecule, respectively.[20] In comparison with the absorption peaks of GOD at 1652 and 1534 cm^{-1}, the little shifts were due to the electrostatic or hydrophobic interaction between protein residues and the mesowalls. The existence of the amide II absorption peak could be a proof of the maintenance of the protein structure,[21] suggesting the good biocompatibility of the nanocage for GOD molecule assembly on the mesowalls and preparation of the biocatalyst. The scheme of the GOD-entrapped nanocage is shown in Figure 6C. Five GOD molecules were arrayed on the mesowall of one nanocage; considering the strong interaction between Pd-MSCF and GOD, GOD would prefer to locate at the mesowalls. Furthermore, the number of GOD molecules arrayed in the nanocage could be controlled by changing the GOD concentration initially used for its assembly.

Optimization of Electrode Preparation and Glucose Detection. To evaluate the potential of the nanocage as a protein entrapment host, several parameters such as the Pd^{2+}-MSCF amount, GOD concentration, and assembly time of GOD for the preparation of the GOD/Pd-MSCF-modified electrode as a glucose biosensor were optimized (Figure 7A−C). The optimization was performed in air-saturated 0.2 M PBS containing 1.0 mM glucose at +0.3 V when the other two factors were at their optimal values. The maximum amperometric response of the GOD/Pd-MSCF-modified electrode to glucose was obtained when the electrode was prepared with 10 μg of Pd^{2+}-MSCF and then immersed in 3.0 mg/mL of GOD solution at pH 5.1 for 140 min. The optimal GOD concentration of 3.0 mg/mL was different from the value of 4.0 mg/mL for maximum entrapment of GOD in Pd^{2+}-MSCF, indicating that the amperometric response depended on both the amount of entrapped GOD and the space left for enzymatic reaction. The suitable space was necessary for access of the substrate to the active sites of the entrapped GOD.

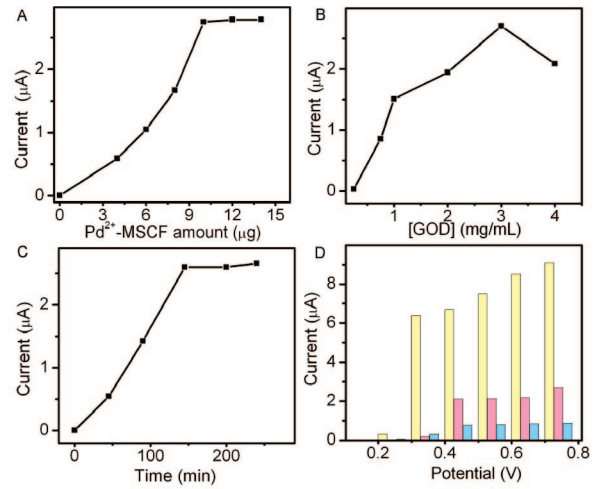

Figure 7. Influences of (A) Pd^{2+}-MSCF amount, (B) GOD concentration, and (C) entrapment time of GOD for the preparation of a GOD/Pd-MSCF-modified electrode and (D) applied potential for amperometric detection on the amperometric response of the modified electrode. The applied potential was chosen by considering the amperometric response of the modified electrode to 2.5 mM glucose (yellow), 0.05 mM AA (cyan), and 0.05 mM AP (magenta). The concentrations of AA and AP were selected according to the concentration ratios of glucose to AA and AP in practical serum samples.

With the increasing applied potential, the amperometric response of the GOD/Pd-MSCF-modified electrode to glucose increased. The high potential was disadvantageous to excluding interference in practical application. As shown in Figure 7D, the responses of ascorbic acid (AA) and acetaminophen (AP) increased when the applied potential changed from +0.3 to +0.7 V. At the applied potential of +0.3 V, their responses were 4.7% and 2.7% of the glucose response at the concentration ratios of AA and AP to glucose in practical serum samples, respectively, while the response of glucose increased by about 23 times when the applied potential changed from +0.2 to +0.3 V. Although the response of glucose slightly increased from 6.41 to 6.69 μA when the applied potential changed from +0.3 to +0.4 V, the responses of AA and AP increased to 11.2% and 31.7% of the glucose response. Thus, +0.3 V was selected for the detection of glucose, at which the interferences from AA and AP were negligible.

Biosensing Application of the GOD/Pd-MSCF-Modified Electrode. Figure 8A shows the amperometric response of the biosensor to 1.0 mM glucose, which was about 65 times that of the GOD/MSCF-modified electrode to 2.0 mM glucose. Thus, the presence of PdNPs improved the sensitivity by about 130 times due to the high catalytic activity of the PdNPs for the electrooxidation of H_2O_2 generated in the enzymatic reaction. The biosensor showed a surprisingly fast response, which achieved a 95% steady-state current in less than 3 s and a linear range from 5.0 μM to 4.0 mM with a relative coefficient of 0.997 ($n = 17$; Figure 8B) and a limit of detection of 1.0 μM, which was much lower than those glucose biosensors fabricated with MSU-F-C (0.07 mM),[12] MSCF (0.035 mM),[15] and carbon nanotube nanoelectrode

(20) Vinu, A.; Miyahara, M.; Ariga, K. *J. Phys. Chem. B* **2005**, *109*, 6436–6441.
(21) Liu, B.; Hu, R.; Deng, J. *Anal. Chem.* **1997**, *69*, 2343–2346.

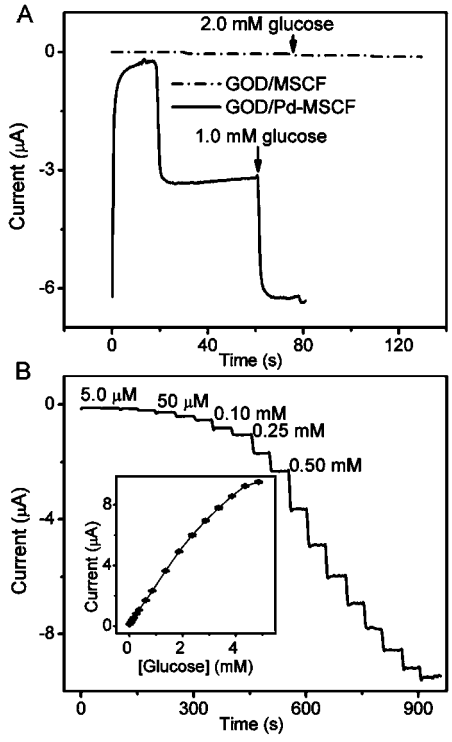

Figure 8. Amperometric response of GOD/Pd-MSCF to glucose. (A) Current–time curves of GOD/Pd-MSCF- and GOD/MSCF-modified electrodes to additions of glucose and (B) GOD/Pd-MSCF-modified electrode to additions of glucose, with the marked concentrations in stirring air-saturated 0.2 M PBS (pH 7.0) at +0.3 V. The inset in B shows a plot of current vs glucose concentration.

ensembles (0.08 mM),[22] respectively. The sensitivity was 2.12 μA/mM, which was also much higher than that obtained at the poly(pyrrole)/tetrathiafulvalene-tetracyanoquinodimethane-based biosensor (70 nA/mM)[23] and was comparable with that of 2.11 μA/mM at a platinum nanoparticles-MWCNT-modified electrode.[24]

At high glucose concentrations, the response showed characteristics of the Michaelis–Menten kinetic mechanism. The apparent Michaelis–Menten constant (K_M^{app}) was calculated to be 0.93 mM[25] (Figure 9), where I_{cat} was the steady-state response to the added substrate at concentration C. This value was lower than 7.8 mM for GOD bound to a redox polymer−carbon-nanotube-modified electrode,[26] and 27 mM for native GOD in solution.[27] The high affinity and fast response of the assembled GOD to its substrate indicated improved enzyme accessibility for achieving high catalytic activity.

The decrease in the overpotential for oxidation of H_2O_2 was beneficial for improving the analytical performance of the glucose biosensor for practical application. At +0.3 V, the interferences from AA and AP were negligible (Figure 7D), and uric acid did not show any response at their concentrations coexisting in the real serum sample.

(22) Lin, Y. H.; Lu, F.; Tu, Y.; Ren, Z. F. *Nano Lett.* **2004**, *4*, 191–195.
(23) Palmisano, F.; Zambonin, P. G.; Centonze, D.; Quinto, M. *Anal. Chem.* **2002**, *74*, 5913–5918.
(24) Hrapovic, S.; Liu, Y.; Male, K.; Luong, J. J. *Anal. Chem.* **2004**, *76*, 1083–1088.
(25) Kamin, R. A.; Wilson, G. S. *Anal. Chem.* **1980**, *52*, 1198–1205.
(26) Joshi, P. P.; Merchant, S. A.; Wang, Y.; Schmidtke, D. W. *Anal. Chem.* **2005**, *77*, 3183–3188.
(27) Rogers, M. J.; Brandt, K. G. *Biochemistry* **1971**, *10*, 4624–4630.

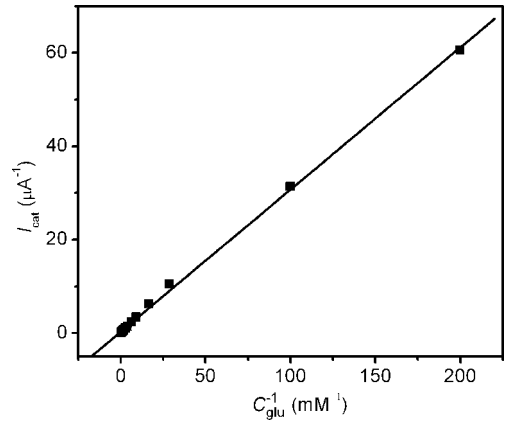

Figure 9. Lineweaver–Burk plot.

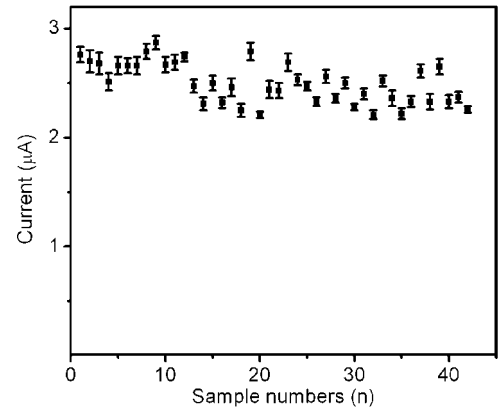

Figure 10. Amperometric responses of 1.0 mM glucose in 42 samples detected at different times.

Reproducibility and Stability for Detection of Glucose. The biosensor had a good reproducibility with a relative standard deviation of 7.6% for the detection of 42 glucose samples at a concentration of 1.0 mM (Figure 10). The 3-D bottleneck structure could more efficiently retain the entrapped GOD than the straight channels of mesoporous materials due to the spatial limitation. The electrostatic and hydrophobic interactions between GOD and the silanols and carbon, respectively, and the strong interactions between the nitrogen groups in GOD molecules and the homogeneously dispersed palladium nanoparticles on the mesowalls[16] could prevent the leakage of the assembled GOD. Thus, the biosensor showed good stability.

Figure 11 shows the amperometric response of the biosensor successively monitored in both static and vigorously stirred 0.1 M PBS containing 1.0 mM glucose at room temperature. In the static case, the response could remain a steady value for 1 week, but it decreased to 74.2% of its initial value after 10 days, while GOD dissolved in PBS lost 28.5% of its initial activity after being stored at room temperature for 10 days, suggesting that the assembled GOD showed slightly better stability than dissolved GOD. After vigorous stirring for 40 h, both the response and the activity of the biosensor did not show any change, indicating a good stability and retention of the enzyme in the nanocage. Although an obvious decrease was observed after stirring for 80 h possibly due to the leaching, the sensor could maintain more than 95% of its initial response after stirring

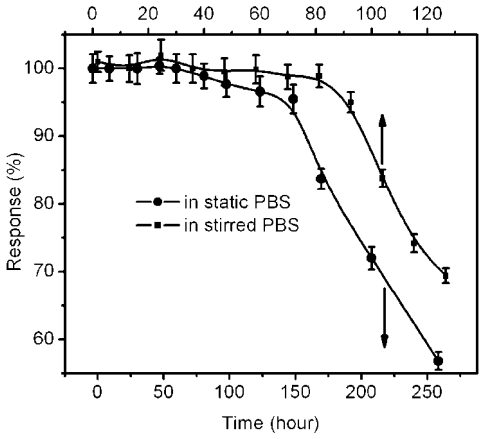

Figure 11. Stability of the GOD/Pd-MSCF-modified electrode monitored at +0.3 V in both static and vigorously stirred 0.1 M PBS containing 1.0 mM glucose.

for 72 h, which was long enough for the detection of glucose *in vivo* or *in vitro*. When the biosensor was stored in the air at 4 °C for 5 weeks, it maintained 89% of its initial response to glucose, which was much better than the values obtained at the $(PDDA/GOx)_n$ multilayer-films-modified GCE/PtC/Nafion enzyme electrode (85% for 1 week),[28] the gold-polypyrrole nanocomposites-modified electrode (60% for two weeks),[29] and the polypyrrole nanotube-array-modified electrode (50% for 14 days),[30] indicating good storage stability due to the biocompatibility of the nanocage.

Conclusion

We have prepared a kind of conductive and biocompatible nanocage of PdNPs deposited on MSCF with high catalytic ability and an ink-bottle-like structure by a designed wet chemical process followed by electrochemical reduction. The diameter of the mesopores can be tuned by adjusting the ratio of two templates. The PdNPs can homogeneously disperse on the mesowalls, show high catalytic activity to electrooxidation of H_2O_2 at a low overpotential, and offer the possibility to selectively detect oxidase substrates. The size-controllable ink-bottle-like nanocage has been used for the size-selective entrapment of GOD, in which GOD molecules are arrayed on the mesowalls, producing a fast response and high affinity to its substrate. The resulting biosensor has high sensitivity, good operational and storage stability, and acceptable selectivity, suggesting that the nanocage is very useful for preparation of highly effective biocatalysts.

Acknowledgment. The authors gratefully acknowledge the National Science Funds for Distinguished Young Scholars (20325518) and Creative Research Groups (20521503), the Key Program (20535010) from the National Natural Science Foundation of China, and the Creative Program for Postgraduates at Jiangsu University for financial support of this research.

CM702906C

(28) Chen, X. J.; Yan, X. B.; Khor, K. A.; Tay, B. K. *Biosens. Bioelectron.* **2007**, *22*, 3256–3260.
(29) Njagi, J.; Andreescu, S. *Biosens. Bioelectron.* **2007**, *23*, 168–175.
(30) Ekanayakeint, E. M. I. M.; Preethichandra, D. M. G.; Kaneto, K. *Biosens. Bioelectron* **2007**, *23*, 107–113.